

Article

The Fate of Trace Elements in Yanshan Coal during Fast Pyrolysis

Jiatao Dang, Qiang Xie *, Dingcheng Liang, Xin Wang, He Dong and Junya Cao

Department of Chemical Engineering, School of Chemical and Environmental Engineering, China University of Mining and Technology (Beijing), D-11 Xueyuan Rd., Haidian District, Beijing 100083, China; dangjt1988@163.com (J.D.); 13810562597@163.com (D.L.); 18010125892@163.com (X.W.); donghe_cumtb@126.com (H.D.); caojy@cumtb.edu.cn (J.C.)

* Correspondence: dr-xieq@cumtb.edu.cn; Tel.: +86-10-6233-1014

Academic Editor: Alireza Somarin

Received: 8 January 2016; Accepted: 31 March 2016; Published: 6 April 2016

Abstract: In this study, a high-sulfur and high-ash yield coal sample obtained from the Yanshan coalfield in Yunnan, China was analyzed. A series of char samples was obtained by pyrolysis at various temperatures (300, 400, 500, 600, 700, 800, and 900 °C) and at a fast heating rate (1000 °C/min). A comprehensive investigation using inductively coupled plasma mass spectrometry (ICP-MS), a mercury analyzer, ion-selective electrode (ISE) measurements, X-ray diffraction (XRD) analysis, and Fourier transform infrared (FTIR) spectroscopy was performed to reveal the effects of the pyrolysis temperature on the transformation behavior of trace elements (TEs) and the change in the mineralogical characteristics and functional groups in the samples. The results show that the TE concentrations in the raw coal are higher than the average contents of Chinese coal. The concentrations of Be, Li, and U in the char samples are higher than those in raw coal, while the opposite was observed for As, Ga, Hg, and Rb. The F and Se concentrations are initially higher but decrease with pyrolysis temperature, which is likely caused by associated fracturing with fluoride and selenide minerals. Uranium shows the highest enrichment degree, and Hg shows the highest volatilization degree compared to the other studied TEs. As the temperature increases, the number of OH groups decreases, and the mineral composition changes; for example, pyrite decomposes, while oldhamite and hematite occur in the chars. It is suggested that the behavior and fate of TEs in coal during fast pyrolysis are synergistically influenced by self-characteristic modes of occurrence and mineralogical characteristics.

Keywords: trace elements; minerals in coal; transformation behavior; coal fast pyrolysis

1. Introduction

Approximately two-thirds of the basic chemical materials in China have been derived from coal or down-stream products. China has been the world's largest coal producer and consumer for several years. The abundance of coal makes it a stable, reliable, and basic fossil energy source for the sustained and rapid development of the Chinese economy and society; for example, approximately 74% of the total primary energy consumption is met by coal [1]. It is anticipated that the utilization of coal will remain stable for a few years in China while a new generation of clean coal technology, especially entrained-flow coal gasification, is being developed to meet global energy demands and to address environmental issues [2].

Coal is a complex flammable rock composed of inorganic and organic material and incorporates almost all of the elements present in the earth's crust. Some potentially toxic and hazardous trace elements (TEs) in coal, such as arsenic, mercury, fluorine, beryllium, and uranium, are thought to pose a potential risk for public health and the natural environment, even if present only at the parts-per-million level. Although the TE concentrations in coal are low, significant emissions of these

pollutants into the environment due to large quantities of anthropogenic coal consumption causes several problems and attracts attention from regulatory authorities and scientists. Coal consumption and related environmental regulations are increasing. Therefore, a detailed investigation of the concentration, distribution, occurrence, and transformation behavior of TEs during coal production, preparation, utilization, and waste disposal is necessary to obtain comprehensive information [3].

There are many studies on the concentration, geochemical, and mineralogical characteristics of TEs in coal [4–10]. For example, Dai *et al.* [11] investigated mineral composition and the TE concentrations in coal from the Huayinshan coalfield. The authors concluded that rare-earth elements mainly occur in rhabdophane and silicorhabdophane, while mercury and selenium are incorporated in pyrite and marcasite. A study by Liu *et al.* [12] showed that U, Mo, Re, Se, Cr, and V are mainly associated with organic components and are less associated with illite or mixed-layer illite/smectite. Extensive work on the partitioning behavior of TEs during coal combustion has been carried out [13,14], such as on the concentration and distribution of TEs in combustion products [15–17], the volatilization or enrichment behavior and chemical composition of TEs in ash [18,19], and the morphology and control technologies of TEs [20,21]. However, information about the behavior and the physical and chemical forms of TEs emitted during coal pyrolysis and gasification is scarce [22]. Several studies address the behavior of TEs during fixed-bed gasification [23,24], fluidized-bed gasification [25], and using other gasification technologies [26–28] employing thermodynamic simulations [29–31]. However, few studies focus on the TE concentration during fast coal pyrolysis [32–34] and entrained-flow coal gasification because simulation experiments are difficult and expensive. Moreover, data are extremely limited with respect to TE behavior during different reaction stages due to the difficulty of analyzing the fate of TEs at various temperatures.

Pyrolysis is an important thermochemical process that can be regarded as both the initial step and/or the accompanying process in most coal conversion processes, such as combustion, gasification, and liquefaction of coal. Furthermore, pyrolysis is a coal-cleaning technology producing fuel or basic chemical materials. Consequently, it is of great importance to analyze the transformation and behavior of TEs during coal pyrolysis. Many of the previous studies on pyrolysis processes were based on low heating rates, which are very different from those in modern coal combustion or gasification processes that are characterized by fast heating.

Hence, the goal of this work is to study coal pyrolysis under fast heating conditions, up to 1000 °C/min, similar to the heating process of modern coal pyrolysis and entrained-flow gasification. We collected a series of Yanshan coal samples from the province of Yunnan in Southwest China, which is enriched with several TEs, such as arsenic, fluorine, gallium, mercury, lithium, rubidium, selenium, and uranium, compared with the average contents of Chinese coal [35]. Experiments were conducted at various temperatures with a heating rate of 1000 °C/min, and TE concentrations were analyzed in detail. This research aims to determine the concentration and partitioning of TEs, and to characterize the mineralogical and chemical compositions during the fast pyrolysis of coal at different temperatures, which can provide insights into possible transformation mechanisms and predict the emission characteristics of TEs during gasification. The experimental operating conditions of the present work may not be fully representative of modern coal pyrolysis and entrained-flow gasification. However, the results provide basic theories or suggestions for TE emission and control.

2. Experiments

2.1. Samples

Ganche meager coal from the Yanshan coalfield, located in Yunnan, was collected and used in the present study. The high TE, sulfur, and ash content in this coal make it atypical. The sampling procedure followed the Chinese Standard Method GB 474-2008 [36]. After the coal was air-dried, the samples were crushed and pulverized to obtain particle sizes < 0.074 mm. Fine-grained coal samples were then stored hermetically for experimental use. The characteristics of the Yanshan coal

are shown in Table 1. The coal ash was sampled at 815 °C, in accordance with the procedure described in the Chinese Standard Method GB/T 212-2008 [37]. X-ray fluorescence spectrometry (PANalytical Axios-Max, Almelo, The Netherlands) was employed to measure the concentrations of major element oxides in the coal ash sample [38]. The results are shown in Table 2.

Table 1. Proximate and ultimate analysis of the coal sample.

Sample	Proximate Analysis %					Ultimate Analysis %			
	M _{ad}	A _d	V _{daf}	FC _{daf}	C _{daf}	H _{daf}	O _{daf}	N _{daf}	S _{t,daf}
Yanshan Coal	3.32	40.98	17.32	82.68	77.97	3.25	1.72	1.08	15.98

M, moisture; A, ash yield; V, volatile matter; FC, fixed carbon; ad, air-dry basis; S_t, total sulphur; d, dry basis; daf, dry and ash-free basis.

Table 2. Concentrations of major element oxides in the coal ash sample.

Sample	Na ₂ O	MgO	Al ₂ O ₃	SiO ₂	SO ₃	K ₂ O	CaO	TiO ₂	V ₂ O ₅	Fe ₂ O ₃
Mass Percentage (%)	0.36	1.60	26.98	54.43	4.15	3.41	3.34	0.78	0.15	4.60

2.2. Pyrolysis Procedure

Approximately 1 g of fine coal samples was weighed and placed into a quartz crucible. Highly pure nitrogen (99.999%) was used to purge the crucible, and the reaction zone was closed. Subsequently, char samples were obtained from pyrolysis at a fast heating rate (1000 °C/min) and at the different pyrolysis temperatures of 300, 400, 500, 600, 700, 800, and 900 °C, in accordance with the procedure by Xie *et al.* [39]. The crucible and reaction zone were heated by a microwave transduction cavity, which can transform the microwave from the workstation into general thermal radiation and can avoid the potential structural influence from the microwave. The final temperature was held for approximately 5 min to complete the pyrolysis. Char samples were weighed again and stored hermetically after the quartz crucible cooled to ambient temperature. The average cooling rate was approximately 45 °C/min before the temperature of the reaction zone was below 200 °C. Char samples were labelled as YCGR-300–900 according to the pyrolysis temperature, while the raw coal sample was labelled as YCGR-000. The char yields of the coal sample at different pyrolysis temperatures are shown in Table 3.

Table 3. Char yields of the coal sample at different pyrolysis temperatures.

Sample	YCGR-300	YCGR-400	YCGR-500	YCGR-600	YCGR-700	YCGR-800	YCGR-900
Char Yield (%)	98.41	97.62	93.25	91.95	89.40	87.31	86.58

2.3. X-Ray Diffraction (XRD) Analysis

Mineralogical characteristics of all of the samples were determined using XRD analysis. The raw coal and char samples were analyzed using a Japanese Rigaku D/max-2500PC X-ray diffractometer (Rigaku Corporation, Tokyo, Japan) with a Cu tube. The XRD pattern was recorded over a 2θ range of 2.5°–70° with a step size of 0.02°. The scanning speed was 4°/min. The accelerating voltage and the tube current of the X-ray diffractometer were 40 kV and 100 mA, respectively.

2.4. Fourier Transform Infrared (FTIR) Spectroscopy

Functional groups and transition characteristics of the raw coal sample as well as the char samples were analyzed using a NICOLET iS-10 FTIR spectrometer (ThermoFisher, Waltham, MA, USA). The KBr disc method was used, with a 1:160 mixture of sample and KBr. Spectra were recorded

in the range of 400–4500 cm^{-1} with an accuracy of 1.929 cm^{-1} . Thirty-two scans were taken with a 4 cm^{-1} spectral resolution.

2.5. TE Analysis

Concentrations of Hg in coal and char samples were determined using a mercury analyzer (DMA-80, Milestone, Sorisole, Italy). Concentrations of F in all of the samples were measured by pyrohydrolysis with an ion-selective electrode (ISE) following the processes stipulated in the ASTM standard. Other TEs, such as arsenic, beryllium, gallium, lithium, rubidium, selenium, and uranium, were determined using inductively coupled plasma mass spectrometry (ICP-MS) (ThermoFisher, X-II) in a three points per peak pulse counting mode. For ICP-MS analysis, a Milestone UltraClave microwave high-pressure reactor was used to digest the samples. The digestion reagents consisted of 5 mL of 65% HNO_3 and 2 mL of 40% HF for each 50 mg of coal, while the solutions consisted of 2 mL of 65% HNO_3 and 5 mL of 40% HF for each 50 mg of non-coal samples. Sub-boiling distillation was used to further purify HF (the Guaranteed Reagent) and HNO_3 (the Guaranteed Reagent) to reduce interferences. Selenium and arsenic contents were measured by ICP-MS using collision-cell technology to eliminate interference due to polyatomic ions. Multi-element standards, such as U in CCS-1, and Be, Ga, and Rb in CCS-4, were used to calibrate the TE concentrations [11,12,40].

3. Results and Discussion

3.1. Effect of Temperature on TE Concentration During Pyrolysis

The TE concentrations of the raw coal sample and the char samples derived from pyrolysis at different temperatures at a fast heating rate are shown in Table 4. The concentrations of Be, Li, and U in all of the chars obtained over the studied temperature range are higher than those of raw coal, while the concentrations of As, Ga, Hg, and Rb of all of the chars obtained are lower than those of raw coal. In contrast, the concentrations of F and Se of some of the char samples are higher than those of raw coal, and others are lower than those of raw coal. The data indicate that Be, Li, and U tend to be enriched in the solid products, whereas As, Ga, Hg, and Rb tend to volatilize during pyrolysis. F and Se are initially enriched in the solid products but then volatilize with increasing temperature. At temperatures lower than 600 °C, F does not show volatilization during fast experimental pyrolysis. The volatility of Hg increases rapidly with increasing temperature in the temperature range below 400 °C and increases slowly above 400 °C because of a surplus shortage. As exhibits a lower volatility than Hg, which may be due to the association with sulfide and silicate minerals. Minimal amounts of volatile TEs, such as As, Hg, and Se, were found in chars compared to raw coal, which indicates that these TEs escape into the gas phase during pyrolysis.

Table 4. Trace element (TE) concentrations in raw coal and chars obtained from pyrolysis at different temperatures.

Sample	As ($\mu\text{g/g}$)	Be ($\mu\text{g/g}$)	F ($\mu\text{g/g}$)	Ga ($\mu\text{g/g}$)	Hg ($\mu\text{g/kg}$)	Li ($\mu\text{g/g}$)	Rb ($\mu\text{g/g}$)	Se ($\mu\text{g/g}$)	U ($\mu\text{g/g}$)
YCGR-000	13.3	1.73	1153	16.1	165	55.9	34.8	25.7	67.6
YCGR-300	11.7	1.95	1194	13.9	98.0	63.6	28.4	26.4	76.2
YCGR-400	11.5	1.95	1252	14.0	19.7	63.7	27.9	24.2	86.6
YCGR-500	12.3	2.04	1270	14.4	4.60	65.8	29.0	26.0	105
YCGR-600	11.9	2.01	1254	14.4	2.87	64.0	29.2	24.5	93.3
YCGR-700	12.5	2.09	1195	15.0	6.84	67.8	30.1	22.9	101
YCGR-800	12.1	2.19	1183	15.0	3.31	69.1	26.1	20.3	124
YCGR-900	11.7	2.32	1141	15.2	4.09	69.8	29.1	19.6	119

A relative parameter (ΔC) is used to clearly and quantitatively describe the changing behavior of TE concentrations in the samples. The value of ΔC was calculated based on the data from Table 3 and is summarized in Figure 1.

$$\Delta C = \frac{c_{chars} - c_{coal}}{c_{coal}} \quad (1)$$

Here, ΔC is the changing rate of concentrations; C_{chars} is the TE concentration in the char samples; and C_{coal} is the TE concentration in the raw coal sample.

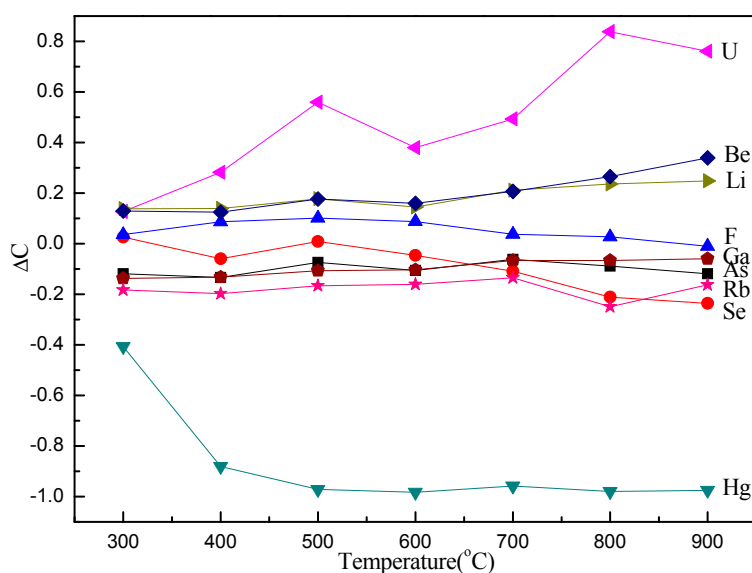


Figure 1. ΔC of trace elements (TEs) in raw coal and char samples obtained from pyrolysis at different temperatures at a fast heating rate.

The enrichment and volatilization of TEs were investigated by introducing a relative parameter (ΔC), which compares the TE content in chars with that in raw coal. Figure 1 presents the ΔC of raw coal and char samples obtained from pyrolysis at different temperatures at a fast heating rate, showing that the ΔC of U, Be, Li, and F is positive, except for F at 900 °C, while the ΔC of Ga, As, Rb, Se, and Hg is negative, except for Se at 300 °C. Uranium shows the highest increase of ΔC , and Hg reveals the largest decrease. It is notable that the enrichment order from high to low is U, Be, Li, and F, and the enrichment of U, Be, and Li increases with increasing pyrolysis temperature, except for F. Mercury almost completely volatilizes at 500 °C and has a much higher volatility than Se, Rb, As, and Ga, even at low temperatures. The volatility of Se is unnoticeable at low temperatures and then increases gradually. The enrichment of Li is very similar to that of Be, and the partitioning of As is similar to that of Se in the samples (Figure 1). The volatility of As, Ga, Hg, Rb, and Se is much higher than that of F, suggesting that a large concentration of these elements is vaporized to the gas phase during pyrolysis.

Studies suggest that the elements associated with the organic matter are more easily vaporized than those associated with minerals, which can hinder TE partitioning into the gas phase. However, there has been no evidence to support that Hg is associated with organic matter in Yanshan coal. The phenomenon of Hg being one of the most volatile TEs in Yanshan coal is likely caused by the Hg characteristics. The conclusion can be drawn that Se, Rb, As, and Ga are volatile TEs during fast pyrolysis, while F has the potential for volatilization at high temperatures, and U, Be, and Li are non-volatile TEs in Yanshan coal. In addition, the behavior of TEs is also influenced by technological parameters, such as reaction atmosphere, mixing status, and product properties. Because of increased

TE emission and the potentially serious risk for the ecosystem environment, more effective measures and countermeasures should be investigated.

3.2. Effect of Temperature on Functional Groups During Pyrolysis

The FTIR spectra of raw coal and char samples obtained from pyrolysis at various temperatures at a fast heating rate are presented in Figure 2. The spectra show well-resolved peaks as IR bands.

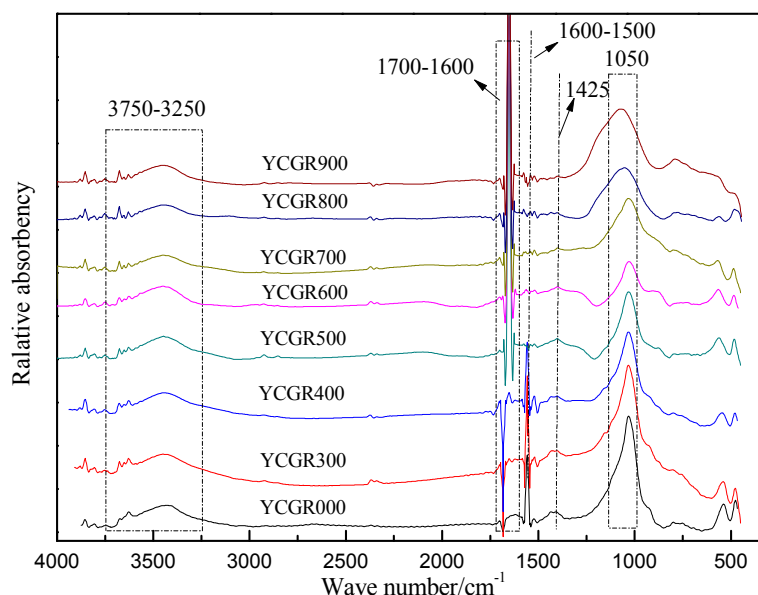


Figure 2. Fourier transform infrared (FTIR) spectra of raw coal and char samples obtained from pyrolysis at different temperatures at a fast heating rate.

It has been reported that some TEs are associated with organic matter or are influenced by organic matter in coal [8,12,41]. Therefore, helpful information may be obtained through an investigation of the changing behavior of the functional groups or organic structure during fast pyrolysis. A band in the region between 3750–3250 cm^{-1} assigned to OH stretching vibrations was observed in all of the samples. However, the band intensity in this region tends to decrease with increasing pyrolysis temperature (Figure 2). The absorbance in this region is attributed to free OH groups, alcohol OH groups, carboxyl OH groups, and the associated OH of aromatic clusters of samples. It is suggested that the OH concentration decreases during pyrolysis. Moreover, a stretching vibration-induced band appears in the region of 1700–1600 cm^{-1} , which is assigned to the aliphatic C=O and -COOH. A small band was observed in the region of 1600–1500 cm^{-1} . This feature, which is assigned to C=C aromatic stretching vibrations of aromatic rings or an aromatic nucleus [42], gradually disappears with the increasing pyrolysis temperature. A possible explanation for these changes is that some aromatic rings in the macromolecular structure of coal or char samples decompose, and a few aliphatic C=O groups are generated from pyrolysis reactions during fast pyrolysis. A notable peak is found in all of the samples at 1050 cm^{-1} due to kaolinite [43]. The peak is sharp in YCGR-000 and then weakens gradually, but it becomes stronger in YCGR-900 compared to the samples obtained at lower temperatures. Calcite stretching vibrations cause a peak at 1425 cm^{-1} [42]. A weak peak at this wave number is found in YCGR-000–600 and disappears in YCGR-700. The possible reason is that calcite decomposes because of the fast heating rate. Note that this also demonstrates the variation of kaolinite and calcite compared to XRD analyses and possibly is a useful source of information about TE migration mechanisms, especially some TEs associated with the organic matter. In general, the peak positions in the FTIR spectra of all of the samples were similar. The difference in absorbance indicates that the quantity and structures of functional groups or minerals changed.

3.3. Effect of Temperature on Mineralogical Characteristics During Pyrolysis

To elucidate the mineralogical characteristics of the samples, XRD patterns of the raw coal and char samples obtained from pyrolysis at various pyrolysis temperatures at a fast heating rate are presented in Figure 3. In raw coal, quartz, mica, gypsum, and pyrite have been identified. The mineralogical characteristics of the char samples from pyrolysis show a minor but interesting variation. The common mineral is quartz, exclusively composed of SiO₂ (Table 2). With increasing temperature, illite, oldhamite, and hematite appear in the chars, which may be due to the transformation of mica, gypsum, and pyrite [44].

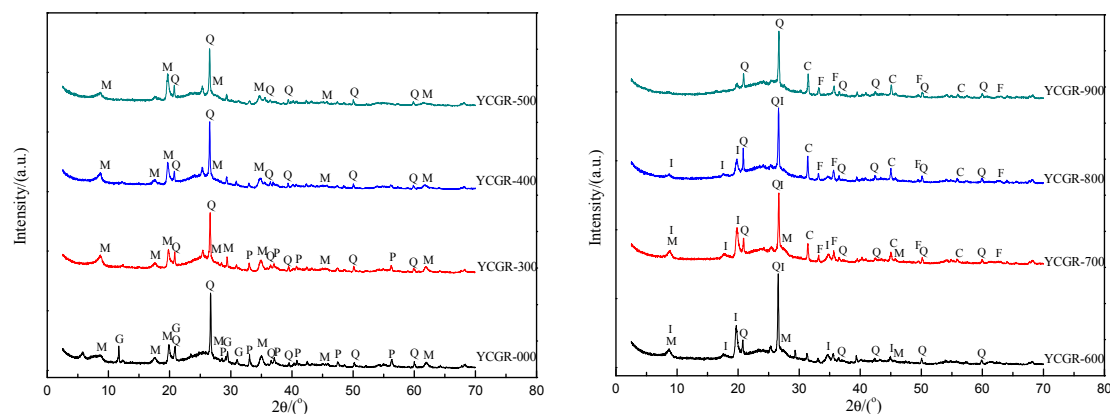


Figure 3. X-ray diffraction (XRD) patterns of raw coal and char samples obtained from pyrolysis at different temperatures at a fast heating rate. Q: quartz; P: pyrite; M: mica (muscovite, polyolithionite, fluorphlogopite); G: gypsum; I: illite; C: oldhamite; F: hematite.

The TE contents are below the detection limit of XRD but are included in many minerals. The results obtained by XRD analysis are in agreement with the behavior of some TEs in the pyrolysis temperatures range. The concentration of F is related to silicate associations [41] and is low in YCGR-900, coincidentally, at the location where fluorphlogopite disappeared in the XRD pattern. It has been reported that most As is associated with pyrite [45,46], and pyrite is found in coal and not in chars, as Figure 3 shows, which provides a possible explanation for the volatilization of As. Minerals identified in chars are different from those in coal, which provides a possible interpretation according to the phenomena of TE enrichment or volatilization. The behavior of TEs during pyrolysis is also related to their characteristics—e.g., Hg expresses higher volatilization than As, although both TEs show similar primary modes of occurrence in coal. Some fluorides and selenides are found in raw coal and char samples, which indicates that there is a competing mechanism of partitioning behavior of F and Se, such as the volatility of F and Se and the hindering influence of minerals. In addition, inorganic cationic matrices, such as iron and calcium, also influence TE atomization [47], which suggests that the partitioning behavior of TEs, such as that of As in Figure 1, is different from the anticipated volatilization degree. Hence, a calcium-based absorber may be useful for the TE solidification in solid products. Research on this phenomenon may be useful to develop environmental pollution control methods and technologies for volatile TEs.

4. Summary and Conclusions

This paper presents a comprehensive study of the influence of different pyrolysis temperatures on TE behavior during coal pyrolysis at a heating rate of 1000 °C/min by analyzing the concentrations of As, Be, F, Ga, Hg, Li, Rb, Se, and U in raw coal and char samples. In addition, the effects of various pyrolysis temperatures on functional groups are investigated to interpret the behavioral characteristics of TEs during fast pyrolysis. The main conclusions drawn are as follows:

(1) The concentrations of As, F, Ga, Hg, Rb, Se, and U are much higher, and the concentration of Li in Yanshan coal is only slightly higher than the average TE values of Chinese coal. However, the raw coal is also very rich in sulfur and ash.

(2) The concentrations of Be, Li, and U in the char samples obtained from pyrolysis are higher than those in raw coal samples. Contrary results are obtained for As, Ga, Hg, and Rb, except for F and Se. The concentrations of F and Se in chars are initially higher but are lower than those in raw coal. The concentration of F in the char sample at 900 °C is lower than that in coal, while a similar phenomenon can be observed when the temperature is above 500 °C for Se, which is likely caused by the association fracturing with fluoride and selenide minerals at this specific temperature.

(3) The enrichment degree of U is much higher than that of the other selected non-volatile TEs, and the volatilization degree of Hg is much higher than that of the other studied volatile TEs. The enrichment of U and the volatilization of Hg increase with increasing pyrolysis temperature. The Hg content changes only slightly above 500 °C, whereas chars show the highest U concentration at 800 °C.

(4) The number of OH groups decreases during fast coal pyrolysis. Interesting changes were also observed regarding the strength of C=O and aromatic rings or aromatic nuclei above 500 °C.

(5) The minerals identified in chars are different from those in coal, which is caused by the pyrolysis reaction and may explain some of the TE behaviors. Pyrite has not been identified in chars, which indicates that As and Hg, associated with or related to pyrite, are being released during pyrolysis. In contrast, oldhamite and hematite are found with increasing pyrolysis temperature. TE partitioning is affected by not only the mode of occurrence in minerals but also the temperature and the element itself. To effectively control TE emission during fast pyrolysis or entrained-flow gasification, further research is necessary.

Acknowledgments: The authors gratefully acknowledge the financial and other support from the National Key Basic Research Program of China (NO. 2014CB238905). The authors also express special and sincere thanks to Shifeng Dai for the kind assistance in the analysis of the concentrations of TEs and to Yuegang Tang for his assistance in the sampling.

Author Contributions: Qiang Xie contributed to the conception of the work. Jiatao Dang, Dingcheng Liang, and Xin Wang performed the pyrolysis experiments. Jiatao Dang, He Dong, and Xin Wang performed the FTIR and XRD experiments. Qiang Xie, Junya Cao, Jiatao Dang, Dingcheng Liang, Xin Wang, and He Dong contributed to the manuscript preparation. Jiatao Dang wrote the manuscript with constructive help from Qiang Xie. All of the authors read and approved the manuscript.

Conflicts of Interest: The authors declare no conflict of interest.

References

1. Dai, S.F.; Ren, D.Y.; Chou, C.L.; Finkelman, R.B.; Seredin, V.V.; Zhou, Y.P. Geochemistry of trace elements in Chinese coals: A review of abundances, genetic types, impacts on human health, and industrial utilization. *Int. J. Coal Geol.* **2012**, *94*, 3–21. [[CrossRef](#)]
2. Li, C.Z. Some recent advances in the understanding of the pyrolysis and gasification behavior of Victorian brown coal. *Fuel* **2007**, *86*, 1664–1683. [[CrossRef](#)]
3. Swaine, D.J. Why trace elements are important. *Fuel Process. Technol.* **2000**, *65*, 21–33. [[CrossRef](#)]
4. Riley, K.W.; French, D.H.; Farrel, O.P.; Wood, R.A.; Huggins, F.E. Modes of occurrence of trace and minor elements in some Australian coals. *Int. J. Coal Geol.* **2012**, *94*, 214–224. [[CrossRef](#)]
5. Dai, S.F.; Ren, D.Y.; Ma, S.M. The cause of endemic fluorosis in western Guizhou Province, Southwest China. *Fuel* **2004**, *83*, 2095–2098. [[CrossRef](#)]
6. Diehl, S.F.; Goldhaber, M.B.; Koenig, A.E.; Lowers, H.A.; Ruppert, L.F. Distribution of arsenic, selenium, and other trace elements in high pyrite Appalachian coals: Evidence for multiple episodes of pyrite formation. *Int. J. Coal Geol.* **2012**, *94*, 238–249. [[CrossRef](#)]
7. Zhao, L.; Ward, C.R.; French, D.; Graham, I.T. Major and trace element geochemistry of coals and intra-seam claystones from the Songzao Coalfield, SW China. *Minerals* **2015**, *5*, 870–893. [[CrossRef](#)]

8. Finkelman, R.B. Modes of occurrence of potentially hazardous elements in coal: Levels of confidence. *Fuel Process. Technol.* **1994**, *39*, 21–34. [[CrossRef](#)]
9. Wang, X.B.; Wang, R.X.; Wei, Q.; Wang, P.P.; Wei, J.P. Mineralogical and geochemical characteristics of Late Permian coals from the Mahe Mine, Zhaoteng Coalfield, Northeastern Yunnan, China. *Minerals* **2015**, *5*, 380–396. [[CrossRef](#)]
10. Vejahati, F.; Xu, Z.H.; Gupta, R. Trace elements in coal: Associations with coal and minerals and their behavior during coal utilization—A review. *Fuel* **2010**, *89*, 904–911. [[CrossRef](#)]
11. Dai, S.F.; Luo, Y.B.; Seredin, V.V.; Ward, C.R.; Hower, J.C.; Zhao, L.; Liu, S.D.; Zhao, C.L.; Tian, H.M.; Zou, J.H. Revisiting the Late Permian coal from the Huayingshan, Sichuan, Southeastern China: Enrichment and occurrence modes of minerals and trace elements. *Int. J. Coal Geol.* **2014**, *122*, 110–128. [[CrossRef](#)]
12. Liu, J.J.; Yang, Z.; Yan, X.Y.; Ji, D.P.; Yang, Y.C.; Hu, L.C. Modes of occurrence of highly-elevated trace elements in superhigh-organic-sulfur coals. *Fuel* **2015**, *156*, 190–197. [[CrossRef](#)]
13. Xu, M.H.; Yan, R.; Zheng, C.G.; Qiao, Y.; Han, J.; Sheng, C.D. Status of trace element emission in a coal combustion process: A review. *Fuel Process. Technol.* **2003**, *85*, 215–237. [[CrossRef](#)]
14. Wang, G.M.; Luo, Z.X.; Zhang, J.Y.; Zhao, Y.C. Modes of occurrence of fluorine by extraction and SEM method in a coal-fired power plant from Inner Mongolia, China. *Minerals* **2015**, *5*, 863–869. [[CrossRef](#)]
15. Swanson, S.M.; Engle, M.A.; Ruppert, L.F.; Affolter, R.H.; Jones, K.B. Partitioning of selected trace elements in coal combustion products from two coal-burning power plants in the United States. *Int. J. Coal Geol.* **2013**, *113*, 116–126. [[CrossRef](#)]
16. Tang, Q.; Liu, G.J.; Zhou, C.C.; Sun, R.Y. Distribution of trace elements in feed coal and combustion residues from two coal-fired power plants at Huainan, Anhui, China. *Fuel* **2013**, *107*, 315–322. [[CrossRef](#)]
17. Roy, B.; Choo, W.L.; Bhattacharya, S. Prediction of distribution of trace elements under oxy-fuel combustion condition using Victorian brown coals. *Fuel* **2013**, *114*, 135–142. [[CrossRef](#)]
18. Oboirien, B.O.; Thulari, V.; North, B.C. Major and trace elements in coal bottom ash at different oxy coal combustion conditions. *Appl. Energy* **2014**, *129*, 207–216. [[CrossRef](#)]
19. James, D.W.; Krishnamoorthy, G.; Benson, S.A.; Seames, W.S. Modeling trace elements partitioning during coal combustion. *Fuel Process. Technol.* **2014**, *126*, 284–297. [[CrossRef](#)]
20. Quick, W.J.; Irons, R.M.A. Trace element partitioning during the firing of washed and untreated power station coals. *Fuel* **2002**, *81*, 665–672. [[CrossRef](#)]
21. Yi, H.H.; Hao, J.M.; Duan, L.; Tang, X.L.; Ning, P.; Li, X.H. Fine particle and trace elements emissions from an anthracite coal-fired power plant equipped with a bag-house in China. *Fuel* **2008**, *87*, 2050–2057. [[CrossRef](#)]
22. Clarke, L.B. The fate of trace elements during coal combustion and gasification: An overview. *Fuel* **1993**, *72*, 731–736. [[CrossRef](#)]
23. Bunt, J.R.; Waanders, F.B. Trace element behavior in the Sasol-Lurgi MK IV FBDB gasifier. Part 1—The volatile elements: Hg, As, Se, Cd and Pb. *Fuel* **2008**, *87*, 2374–2387. [[CrossRef](#)]
24. Bunt, J.R.; Waanders, F.B. Trace element behavior in the Sasol-Lurgi MK IV FBDB gasifier. Part 2—The semi-volatile elements: Cu, Mo Ni and Zn. *Fuel* **2009**, *88*, 961–969. [[CrossRef](#)]
25. Huang, Y.J.; Jin, B.S.; Zhong, Z.P.; Rui, X.; Zhou, H.C. The relationship between occurrence of trace elements and gasification temperature. *Proc. CSEE* **2006**, *26*, 10–15. (In Chinese).
26. Liu, S.Q.; Wang, Y.T.; Yu, L.; Oakey, J. Volatilization of mercury, arsenic and selenium during underground coal gasification. *Fuel* **2006**, *85*, 1550–1558. [[CrossRef](#)]
27. Yoshiie, R.; Taya, Y.; Ichiyangi, T.; Ueki, Y.; Naruse, I. Emissions of particles and trace elements from coal gasification. *Fuel* **2013**, *108*, 67–72. [[CrossRef](#)]
28. Liu, S.Q.; Wang, Y.T.; Yu, L.; Oakey, J. Thermodynamic equilibrium study of trace element transformation during underground coal gasification. *Fuel Process. Technol.* **2006**, *87*, 209–215. [[CrossRef](#)]
29. Duchesne, M.A.; Hall, A.D.; Hughes, R.W.; Mccalden, D.J.; Anthony, E.J.; Macchi, A. Fate of inorganic matter in entrained-flow slagging gasifiers: Fuel characterization. *Fuel Process. Technol.* **2014**, *118*, 208–217. [[CrossRef](#)]
30. Gibbs, B.M.; Thompson, D.; Argent, B.B. A thermodynamic equilibrium comparison of the mobilities of trace elements when washed and unwashed coals are burnt under Pffiring conditions. *Fuel* **2004**, *83*, 2271–2284. [[CrossRef](#)]
31. Diaz-Somoano, M.; Martinez-Tarazona, M.R. Trace element evaporation during coal gasification based on a thermodynamic equilibrium calculation approach. *Fuel* **2003**, *82*, 137–145. [[CrossRef](#)]

32. Guo, R.X.; Yang, J.L.; Liu, D.Y.; Liu, Z.Y. Transformation behavior of trace elements during coal pyrolysis. *Fuel Process. Technol.* **2002**, *77*, 137–143. [[CrossRef](#)]
33. Guo, R.X.; Yang, J.L.; Liu, D.Y.; Liu, Z.Y. The fate of As, Pb, Cd, Cr and Mn in a coal during pyrolysis. *J. Anal. Appl. Pyrolysis* **2003**, *70*, 555–562. [[CrossRef](#)]
34. Guo, R.X.; Yang, J.L.; Liu, Z.Y. Behavior of trace elements during pyrolysis of coal in a simulated drop-tube reactor. *Fuel* **2004**, *83*, 639–643. [[CrossRef](#)]
35. Dai, S.F.; Wang, X.B.; Chen, W.M.; Li, D.H.; Chou, C.L.; Zhou, Y.P.; Zhu, C.S.; Li, H.; Zhu, X.W.; Xing, Y.W.; et al. A high-pyrite semianthracite of Late Permian age in the Songzao Coalfield, Southwestern China: Mineralogical and geochemical relations with underlying mafic tuffs. *Int. J. Coal Geol.* **2010**, *83*, 430–445. [[CrossRef](#)]
36. Standardization Administration of the People's Republic of China. *Method for Preparation of Coal Sample*; Chinese Stand GB/T 474-2008; Standardization Administration of the People's Republic of China: Beijing, China, 2008. (In Chinese)
37. Standardization Administration of the People's Republic of China. *Proximate Analysis of Coal*; Chinese Stand GB/T 212-2008; Standardization Administration of the People's Republic of China: Beijing, China, 2008. (In Chinese)
38. Hower, J.C.; Eble, C.F.; O'Keefe, J.M.; Dai, S.F.; Wang, P.P.; Xie, P.P.; Liu, J.J.; Ward, C.R.; French, D. Petrology, palynology, and geochemistry of Gray Hawk Coal (Early Pennsylvanian, Langsettian) in Eastern Kentucky, USA. *Minerals* **2015**, *5*, 592–622. [[CrossRef](#)]
39. Xie, Q.; Liang, D.C.; Tian, M.; Dang, J.T.; Liu, J.C.; Yang, M.S. Influence of heating rate on structure of chars derived from pyrolysis of Shenmu coal. *J. Fuel Chem. Technol.* **2015**, *43*, 798–908. (In Chinese)
40. Dai, S.F.; Wang, X.B.; Zhou, Y.P.; Hower, J.C.; Li, D.H.; Chen, W.M.; Zhu, X.W.; Zou, J.H. Chemical and mineralogical compositions of silicic, mafic, and alkali tonsteins in the Late Permian coals from the Songzao Coalfield, Chongqing, Southwest China. *Chem. Geol.* **2011**, *282*, 29–44. [[CrossRef](#)]
41. Wang, X.B.; Dai, S.F.; Sun, Y.Y.; Li, D.; Zhang, W.G.; Zhang, Y.; Luo, Y.B. Modes of occurrence of fluorine in the Late Paleozoic No.6 coal from the Haerwsu Surface Mine, Inner Mongolia, China. *Fuel* **2011**, *90*, 248–254. [[CrossRef](#)]
42. Okolo, G.N.; Neomagus, H.W.; Everson, R.C.; Roberts, M.J.; Bunt, J.R.; Sakurovs, R.; Mathews, J.P. Chemical-structural properties of South African bituminous coals: Insights from wide angle XRD-carbon fraction analysis, ATR-FTIR, solid state ¹³C NMR, and HRTEM techniques. *Fuel* **2015**, *158*, 779–792. [[CrossRef](#)]
43. Qin, Z.H.; Chen, H.; Yan, Y.J.; Li, C.S.; Rong, L.M.; Yang, X.Q. FTIR quantitative analysis upon solubility of carbon disulfide/*N*-methyl-2-pyrrolidinone mixed solvent to coal petrographic constituents. *Fuel Process. Technol.* **2015**, *133*, 14–19. [[CrossRef](#)]
44. Tian, C.; Zhang, J.Y.; Zhao, Y.C.; Gupta, R. Understanding of mineralogy and residence of trace elements in coals via a novel method combining low temperature ashing and float-sink technique. *Int. J. Coal Geol.* **2014**, *13*, 162–171. [[CrossRef](#)]
45. Huggins, F.E.; Huffman, G.P. Modes of occurrence of trace elements in coal from XAFS spectroscopy. *Int. J. Coal Geol.* **1996**, *32*, 31–53. [[CrossRef](#)]
46. Dai, S.F.; Zeng, R.S.; Sun, Y.Z. Enrichment of arsenic, antimony, mercury, and thallium in a Late Permian anthracite from Xingren, Guizhou, Southwest China. *Int. J. Coal Geol.* **2006**, *66*, 217–226. [[CrossRef](#)]
47. Raeva, A.A.; Dongari, N.; Artemyeva, A.A.; Kozliak, E.I.; Pierce, D.T.; Seames, W.S. Experimental simulation of trace element evolution from the excluded mineral fraction during coal combustion using GFAAS and TGA-DSC. *Fuel* **2014**, *124*, 28–40. [[CrossRef](#)]

